JOURNAL OF APPLIED ELECTROCHEMISTRY 23 (1993) 125–134

Aluminium alloys in sulphuric acid Part I: Electrochemical behaviour of rotating and stationary disc electrodes

F. HOLZER, S. MÜLLER, J. DESILVESTRO*, O. HAAS

Paul Scherrer Institute (PSI), CH-5232 Villigen PSI, Switzerland

Received 13 April 1992; revised 25 June 1992

Anodic oxidation of various aluminium alloys was investigated by means of rotating disc electrodes in 3 M H_2SO_4 as a function of Cl^-, F^-, Zn^{2+} and In^{3+} concentration. Al–In, Al–Zn/In and Al–Zn/Sn alloys yielded current–potential curves at the lowest overpotentials and faradaic efficiencies for anodic oxidation of up to 98% at currents $\geqslant 50\,mA\,cm^{-2}$. While these alloys were electrochemically active in the presence of chloride as the only additive in sulphuric acid, binary aluminium alloys with Ce, Ga, La, Nd, Sn, Ta, Te, Ti or Tl were only active when Cl^-, Zn^{2+} and In^{3+} species were added to the electrolyte. With the exception of Al–Ga, binary alloys displayed high faradaic efficiencies of up to 95%. Fluoride additives resulted in current–potential curves at even more negative potentials than those with chlorides. In contrast to Cl^-, fluoride ions are consumed during the aluminium oxidation process due to complexation with Al(III).

1. Introduction

Aluminium is a unique metal with attractive properties for energy storage such as low equivalent weight (9 g per faraday), large natural resources and a fairly low price (about $1300 per ton, [1]). In comparison to other high energy density materials, e.g. hydrogen, sodium or lithium, aluminium can be handled and stored easily and safely. From all presently known devices for electricity production from aluminium, aluminium/air batteries appear to be the most promising. Aluminium/air batteries employing alkaline [2–4] or neutral electrolytes [5–7] have been developed to a state of commercialization. Although corrosion rates have been lowered significantly over the last 30 years by proper choice of aluminium alloy and control of impurities [4], large scale application of aluminium/air batteries is still encumbered by some inherent problems with aluminium in aqueous electrolytes. Power densities are rather low ($< 50\,W\,dm^{-3}$), especially when neutral electrolytes are employed. Due to the negative thermodynamic potential of Al, aluminim batteries employing aqueous electrolytes cannot be recharged electrically, however, mechanical replacement of electrodes and electrolyte may offer the advantage of fast rechargeability. Efficient precipitation and separation of aluminium hydroxides from the electrolyte represents one of the major problems. In addition, oxygen diffusion electrodes show poor long term behaviour, partly due to precipitation of carbonates from alkaline solutions originating from CO_2 from air. Therefore, CO_2 scrubbing may be required for the operation of aluminium/air cells with alkaline elecrolytes.

Based on the aluminium corrosion rate [8], pH values of 2–10 would be most advantageous for battery operation. In previous studies [9, 10], we showed that aluminium can be used in saline electrolytes of pH 2–4 in combination with suitable additives (Zn^{2+}, In^{3+} or Hg^{2+}). High faradaic efficiencies of up to 95% and currents of $100\,mA\,cm^{-2}$ were achieved at potentials only 0.5–0.75 V more positive than the thermodynamic Al^{3+}/Al potential. The same electrolytes were used for the operation of a 200 W Al/Cl_2 battery developed in our laboratory [11, 12].

Similarly to neutral solutions, weakly acidic electrolytes have the disadvantage of rather large pH excursions and thus potential drifts, especially at the oxygen electrode. Some of the problems encountered with alkaline, neutral or weakly acidic electrolytes may be avoided by employing *highly acidic* solutions. Such electrolytes offer CO_2 compatibility of the air electrode, higher electrolytic conductivities and, therefore, better power capabilities. Aluminium salts, for example sulphates, may be separated from the electrolyte by precipitation or ion exchange.

It is known that HCl solutions, for instance, give rise to high aluminium corrosion rates [9, 13]. In this work we therefore attempted, on the one hand, to exploit the passivating character of sulphuric acid in order to suppress non-faradaic aluminium oxidation. On the other hand, we investigated the selective activating effect of various additives in the alloy and in the electrolyte. Alloys were selected on the basis of either their known activating properties in alkaline and neutral solutions (e.g. Al + Ga, In, Sn, Tl, Zn [3–7, 14–26]) or the improved corrosion resistance of

* Present address: Leclanché S.A., 48, Avenue de Grandson, CH-1400 Yverdon-les-Bains, Switzerland

0021-891X

aluminium alloys with refractory metals (e.g. Al + Ta, Ti, Nb [27–29]). Aluminium alloys were characterised by current-potential curves and faradaic efficiencies for aluminium oxidation in 3 M H_2SO_4 with various additives in the electrolyte in order to rate their suitability as anode materials in aluminium/air batteries with acidic electrolytes [30, 31].

2. Experimental details

2.1. *Anodes*

High purity aluminium (Al 99.999%) was obtained from Aldrich. All aluminium alloys are based on Al 99.99% and were kindly provided by Alusuisse-Lonza Services AG, Switzerland. The following alloys were employed in this investigation (percentages are by weight): Al–Ce 0.05 and 0.20%, Al–Ga 0.05 and 0.10%, Al–In 0.10%, Al–La 0.10 and 0.20%, Al–Nd 0.10 and 0.29%, Al–Sn 0.50%, Al–Ta 0.10 and 0.50%, Al–Te 0.014 and 0.015%, Al–Ti 0.50 and 1.2%, Al–Tl 0.086 and 0.16%, Al–Zn/In (3.3%/0.025%), Al–Zn/Sn (6.5%/0.16%).

Rotating disc electrodes were fabricated by mounting a 16 mm diameter aluminium rod (2.0 cm^2) in a Kel-F sheath of 20 mm outer diameter. Aluminium working electrodes were polished mechanically, successively with Buehler 180, 240, 320, 400 and 600 SiC papers.

2.2. *Electrolytes*

Electrochemical experiments were carried out in 3 M H_2SO_4 (diluted from concentrated H_2SO_4, Baker Chemicals, p.A.) with various additives. $ZnSO_4 \cdot 7H_2O$, $ZnCl_2$, KF and $Al_2(SO_4)_3 \cdot 18H_2O$ were obtained from Merck (p.a. quality) and $In_2(SO_4)_3 \cdot 5H_2O$ (purum) from Fluka. The total chloride concentration was adjusted by addition of HCl (Baker Chemicals, p.A.). All chemicals were used as received.

2.3. *Apparatus*

Current-potential curves were measured in a Metrohm cell with an electrolyte volume of 50 ml. A Hg/Hg_2SO_4 reference electrode was positioned a few millimetres below the working electrode. A platinum sheet was used as the counter electrode. Electrochemical measurements involved an AMEL Model 555B potentiostat and an AMEL Model 568 function generator. Currents were integrated with an AMEL Model 731 integrator. Unless otherwise noted, potentials are quoted with respect to Hg/Hg_2SO_4 (0.64 V/NHE).

Faradaic efficiencies were determined from the electric charge and from the weight loss during anodic aluminium oxidation for 4 h under potentiostatic control. The cell consisted of two compartments, separated by a cellophane membrane. Each compartment contained about 200 ml electrolyte solution. The working and the reference electrode (a few millimetres apart) were placed in one compartment and the platinum counter electrode in the other one. The measurements were performed with rotating and stationary disc electrodes. The surface of rotating electrodes was oriented horizontally while the stationary electrodes were arranged vertically in order to allow hydrogen bubbles to escape.

3. Results and discussion

3.1. *Current–potential curves*

The electrochemical behaviour of aluminium anodes in 3 M H_2SO_4 was characterized by current–potential curves of rotating disc electrodes (rotation rate = 1500 r.p.m.), employing various alloys and additives in the electrolyte. In previous work with weakly acidic NaCl electrolytes (pH 1–4), we showed that submillimolar amounts of In(III) in combination with Zn(II) (ca. 80 mM) resulted in efficient surface activation for anodic aluminium oxidation [9]. High faradaic efficiencies of 90–95% were obtained (i.e. 10–5% hydrogen evolution) for the pH range 2–3. With the same additives in 3 M H_2SO_4 however, pure aluminium and all alloys tested could not be activated due to the strongly passivating character of H_2SO_4. Therefore small amounts of a halogenide, usually 40 mM HCl, were added to 3 M H_2SO_4. Further addition of Zn(II) and In(III) compounds shifted the current–potential characteristics towards more negative values in most experiments. Additive concentrations were optimized in a variety of experiments in order to obtain stable oxidation currents at potentials as negative as possible. As a rule, a threshold concentration of Cl^-, Zn^{2+} or In^{3+} was required to observe any significant effect. Above certain concentration limits on the other hand, no further improvement was obtained. The optimised conditions were found to be 40 mM chloride and, depending on the alloy, addition of 0.5–1 mM In(III) and/or 10–80 mM Zn(II).

3.1.1. Influence of chloride, Zn(II), In(III) additives on pure Al.. Pure aluminium (99.999%) is electrochemically passive in sulphuric acid, with almost zero anodic currents. Addition of HCl (40 mM) to 3 M H_2SO_4 resulted in a large current increase at potentials > -0.9 V during a potentiodynamic scan (Fig. 1a). The current–potential loop observed upon scan reversal (—— in Fig. 1a), as well as the current increase while maintaining the electrode potential at -1.0 V during an anodic scan (– – – in Fig. 1a), can be rationalized by chloride ion induced piting which activates the electrode surface for anodic oxidation. Aluminium corrosion in chloride medium has been investigated extensively, employing electrochemical techniques [32], a.c. impedance [35–37], electron microscopy [36–39], radio tracer experiments [40], Auger and XPS [41, 42] or AC quartz electrogravimetry [37].

Addition of chloride (40 mM) and Zn(II) (80 mM) resulted in a similar voltammogram (Fig. 1b), however with an anodic peak at about -1.36 V due to Zn oxidation ($E°[Zn/Zn^{2+}] = -1.40$ V (Hg/Hg_2SO_4)).

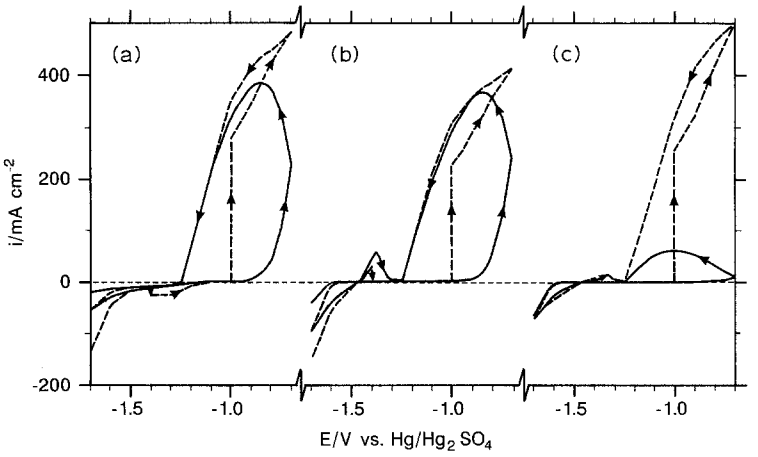

Fig. 1. Current-potential curves for an Al 99.999% anode in 3 M H_2SO_4 with different additives. Scan rate was 10 mV s^{-1} (—— cycle 1, - - - cycle 2), rotation rate 1500 r.p.m. Additives employed: 40 mM HCl (a), 20 mM $ZnCl_2$ + 60 mM $ZnSO_4$ (b) and 20 mM $ZnCl_2$ + 60 mM $ZnSO_4$ + 0.25 mM $In_2(SO_4)_3$ (c). The anodic scan of the second cycle was halted at – 1.4 V and – 1.0 V until the current density reached a stable value.

During prolonged polarization at potentials > – 1.4 V, the currents decayed to zero (- - - in Fig. 1b), indicating a depletion of zinc from the surface. Submillimolar amounts of In(III) (0.5 mM) added to 3 M H_2SO_4 + HCl + Zn(II) resulted, for pure aluminium, in no significant improvement of current–potential characteristics under potentiodynamic conditions (Fig. 1c), in contrast to certain alloys (see below) or pure aluminium in 2 M NaCl at pH 2 [9]. However, anodic currents at a given potential were more stable when In(III), as well as chloride and Zn(II), were employed as additives.

3.1.2. Al–In, Al–Zn/In, Al–Zn/Sn alloys. Figure 2 shows the effect of electrolyte additives on the current–potential characteristics of an Al–Zn/In alloy electrode. In the case of 3 M H_2SO_4 + 40 mM HCl (Fig. 2a), the onset of anodic oxidation occurred at a lower overpotential than with pure aluminium (Fig. 1a). While the first anodic scan still occurred at fairly positive potentials, the current-potential curve was shifted to significantly more negative potentials (by about 0.5 V) after scan reversal. Reproducible current–potential curves displaying almost no hysteresis between anodic and cathodic scan were obtained after several cycles between – 1.7 and – 1.0 V in 3 M H_2SO_4 + 40 mM HCl electrolytes. At a given potential, the currents were significantly higher than in the case of chloride induced pitting corrosion on pure aluminium. In accordance with work on aluminium activation in alkaline and neutral electrolytes [4, 43], such behaviour is referred to as 'superactivity' in this paper. In the case of HCl + Zn(II) (Fig. 2b) or HCl + Zn(II) + In(III) (Fig. 2c) as additives, superactivation occurred after even fewer cycles and resulted in current-potential curves at slightly more negative potentials. When all three additives were used, practically no induction time was necessary for electrode activation.

Current–potential curves were also recorded under galvanostatic control, monitoring steady-state potentials as a function of current. Readings were taken when the potential varied by less than 5 mV within 1 min. In Fig. 3, current–potential curves of the alloys Al–In 0.10, Al–Zn/In and Al–Zn/Sn are shown for 3 M H_2SO_4 + 40 mM HCl. Pure aluminium in comparison, yielded stable potentials only when choride, Zn(II) and In(III) were used as additives. As shown in

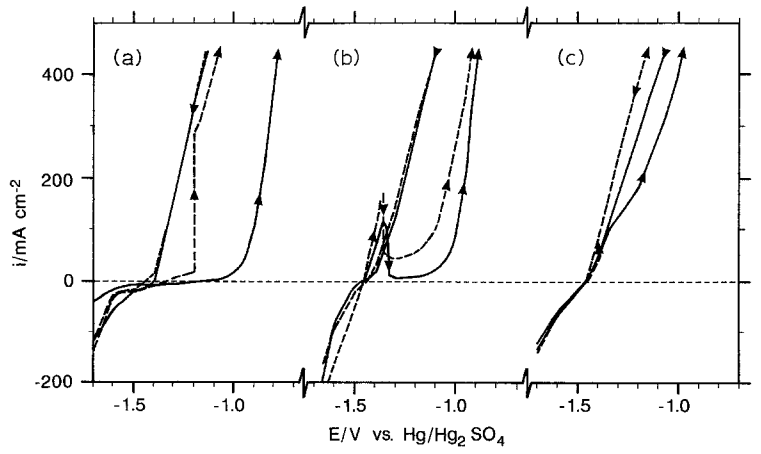

Fig. 2. Current potential curves for an Al–Zn/In electrode in 3 M H_2SO_4 with different additives. Scan rate was 10 mV s^{-1} (—— cycle 1, - - - cycle 2), rotation rate 1500 r.p.m. Additives employed: 40 mM HCl (a), 20 mM $ZnCl_2$ + 60 mM $ZnSO_4$ (b) and 20 mM $ZnCl_2$ + 60 mM $ZnSO_4$ + 0.25 mM $In_2(SO_4)_3$ (c). The anodic scan of the second cycle was halted at – 1.4 V and – 1.0 V until the current density reached a stable value.

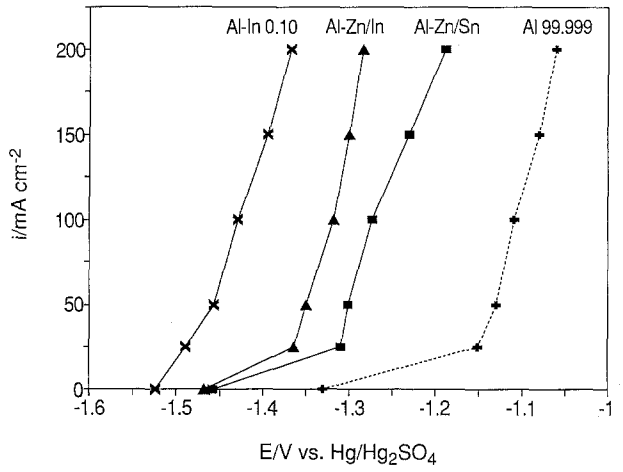

Fig. 3. Galvanostatically recorded current-potential curves of Al–In 0.10 (x), Al–Zn/In (▲) and Al–Zn/Sn (■) in 3 M H_2SO_4 with 40 mM HCl as the only additive. Rotation rate was 1500 r.p.m. Al 99.999 (+): 3 M H_2SO_4 + 20 mM HCl + 10 mM $ZnCl_2$ + 0.5 mM $In_2(SO_4)_3$ (without Zn^{2+} and In^{3+} the potential of Al 99.999 increased steadily to values up to > 10 V due to passivation). Galvanostatic measurements were performed after two potentiodynamic cycles between −1.7 V and −0.7 V as described in Figs 1 and 2.

Fig. 3, overpotentials were significantly lower for the three alloys in the presence of 40 mM chloride (superactivation), compared to pure aluminium with all three electrolyte additives. The potential shift increased in the order Al–Zn/Sn < Al–Zn/In < Al–In 0.10 and amounted to 0.15–0.35 V. Our data suggests that from all alloying elements employed in this work, indium exerts the largest superactivating effect in strongly acidic electrolytes.

The onset potential for anodic oxidation of −1.53 V for Al–In 0.10 corresponds to −0.89 V NHE which is about 0.77 V more positive than the thermodynamic Al^{3+}/Al potential of −1.66 V/NHE [8]. Anodic currents of 100 mA cm^{-2} were obtained with suitable aluminium alloys in H_2SO_4 based electrolytes at overpotentials ≤ 0.85 V (note that current-potential curves were not corrected for uncompensated electrolyte resistance). These overvoltages compare favourably to values reported for superactive alloys in alkaline electrolytes, for example about 0.95 V for Al–Sn alloys at a current density of 100 mA cm^{-2} [4].

Figures 4(a) and (b) show the influence of electrolyte additives on anodic oxidation of Al–Zn/Sn and on Al–In 0.10 in comparison to Al 99.999 (the latter with all three additives in the electrolyte). The extent of superactivation as a function of additives in the electrolyte depends very much on the alloy. In the case of Al–Zn/Sn (Fig. 4a), almost no difference was observed between 3 M H_2SO_4 + HCl (x) and 3 M H_2SO_4 + HCl + Zn(II) (▲). This finding is not surprising since the Al–Zn/Sn alloy contains 6.5 wt % Zn which is expected to be anodically oxidised at potentials > −1.4 V. Addition of HCl, Zn(II) and In(III) (■) however, induced a negative potential shift of 0.1–0.15 V compared to Zn(II) and/or HCl additives.

A fairly different dependence of electrolyte additives was observed for Al–In 0.10 (Fig. 4b). For this alloy, the most active behaviour was obtained when HCl was the only additive in the electrolyte (x), while more

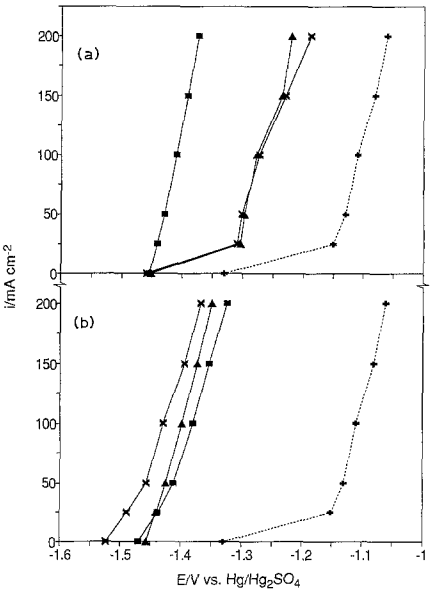

Fig. 4. Galvanostatically recorded current-potential curves of Al–Zn/Sn (a, ——), Al–In 0.10 (b, ——) and Al 99.999 (a, b, ····) in 3 M H_2SO_4 with different additives: 40 mM HCl (x), 20 mM $ZnCl_2$ + 60 mM $ZnSO_4$ (▲), 20 mM $ZnCl_2$ + 60 mM $ZnSO_4$ + 0.25 mM $In_2(SO_4)_3$ (■) and 20 mM HCl + 10 mM $ZnCl_2$ + 0.5 mM $In_2(SO_4)_3$ (+). Rotation rate was 1500 r.p.m.

positive potentials were observed when all three additives were employed (■). In comparison to the Al–Zn/Sn alloy (Fig. 4a), the differences between the various additives were less pronounced, indicating that the main activating power stems from indium in the alloy and not from the additives in the electrolyte.

Similarly to Al–In 0.10 (Fig. 4b), Al–Zn/In displayed only small differences in potential shift between the different electrolyte additives (no Figure shown). The corresponding three curves were shifted by 0.01–0.05 V towards more positive potentials in comparison to the curve (■) in Fig. 4b for Al–In 0.10, showing that the Al–Zn/In alloy is slightly less active than Al–In 0.10. The activating tendency, was, in analogy to the Al–Zn/Sn alloy, highest when HCl + Zn(II) + In(III) were employed as additives (cf. Fig. 2).

3.1.3. Other aluminium alloys. In addition to Al–In 0.10, Ph–Zn/In and Al–Zn/Sn alloys, also Al–Ga 0.10 and 0.05 displayed current-potential curves with onset potentials between −1.4 V and −1.5 V, however only in the presence of chloride, Zn(II) and In(III). All other alloys tested, i.e. Al–Ce, –La, –Nd, –Sn, –Ta, –Te, –Ti, –Tl, yielded stable currents of > 20 mA cm^{-2} only at potentials more positive than −1.15 V to −1.1 V, and only when chloride, Zn(II) and In(III) were used as additives. These potentials are 0.3–0.4 V more positive than those of superactive alloys employed in this work and about 1.2 V more positive than the thermodynamic Al^{3+}/Al potential.

For a technical grade aluminium alloy we obtained even lower overpotentials when submillimolar amounts of Hg(II) were added to 2 M NaCl of pH 2 (onset potential for anodic aluminium oxidation at about 0.4 V against Al^{3+}/Al, [10]), in comparison to Zn(II) and In(III) additives in the same saline electrolyte [9]. Because of rather high corrosion rates (faradaic

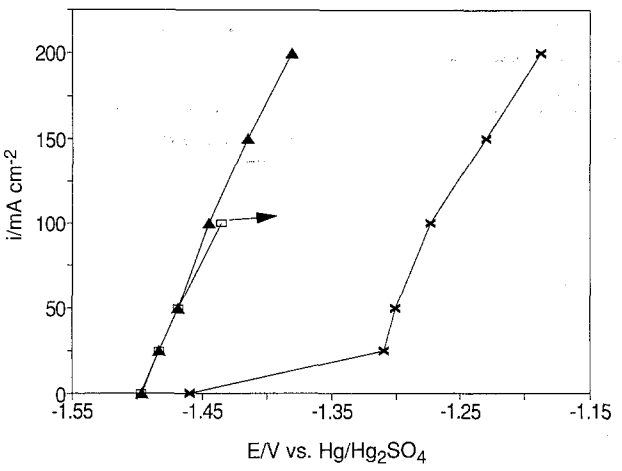

Fig. 5. Galvanostatically recorded current-potential curves of Al–Zn/Sn in 3 M H_2SO_4 with fluoride and chloride additives. 40 mM KF (□), 60 mM KF (▲), 40 mM HCl (x). At currents higher than 100 mM cm^{-2} the electrode passivated in 3 M H_2SO_4 + 40 mM KF. Rotation rate was 1500 r.p.m.

efficiencies of only 62–77%, [10]) and environmental considerations, Hg(II) additives were, however, not investigated in this work.

3.1.4. Influence of fluoride additives. The effect of fluoride in comparison to chloride on the Al–Zn/Sn alloy is shown in Fig. 5. Replacement of HCl (40 mM, x) by KF (40 mM, □) resulted in a shift of the current–potential characteristics to more negative potentials (by about 0.18 V). However, the electrode passivated at currents $> 100\,mA\,cm^{-2}$, reaching potentials > 2 V. A KF concentration of at least 60 mM was needed in order to obtain stable currents up to $200\,mA\,cm^{-2}$ (▲ in Fig. 5, rotation rate = 1500 r.p.m.). Since fluoride ions form much stronger complexes with Al(III) than chloride ions [44] the diffusion layer is depleted of F^- above a certain current level. Passivation also occurred when aluminium sulphate was added (e.g. 100 mM Al(III), showing that dissolved Al(III) strongly binds F^-. 160 mM KF was needed to restore active behaviour up to $200\,mA\,cm^{-2}$ in the case of 100 mA Al(III), and 280 mM KF was required when the total Al(III) concentration was 200 mM. Such behaviour was not seen with chloride additives, where stable currents were obtained in the presence of 40 mM chloride with Al(III) concentrations of up to 1.5 M Al(III) [31]. However, similar activation/passivation effects at open circuit and under anodic polarization, respectively, have also been observed in neutral NaF or mixed NaF/NaCl solutions [45].

Based on the dissociation constant of HF (3.53×10^{-4}, [46]) and the complex formation constants for $AlF_n^{(3-n)+}$ ($n = 1 - 4$, [44]), bulk concentrations of free F^-, HF and the various Al(III) species were calculated (Table 1). Very low free fluoride concentrations of $F^- \geqslant 8 \times 10^{-6}$ M in the bulk are obviously sufficient for electrode activation when no Al(III) is present in the bulk electrolyte. F^- concentrations in Al(III) containing electrolytes (lines 3 and 4 in Table 1) are even lower due to effective complexation. It therefore appears that also AlF^{2+} and AlF_2^+ species are partly responsible for electrode activation, since they are expected to be the main species in the diffusion layer during anodic aluminium oxidation. Despite the more efficient surface activation by fluorides, these additives are not appropriate for battery applications because of stoichiometric consumption during anodic aluminium oxidation (1–3 F^- per Al) and also due to their toxicity.

3.2. *Faradaic efficiencies*

In order to be suitable as an anode material in an aluminium battery with aqueous electrolytes, the alloy should display on the one hand a current-potential characteristics at sufficiently negative potentials (high superactivity) and on the other hand minimum hydrogen evolution due to parasitic corrosion. Based on current–potential characteristics alone (section 3.1.), Al–Ga, Al–In, Al–Zn/In or Al–Zn/Sn alloys would be most promising for battery applications. In this section, also the corrosion behaviour of the alloys studied in 3.1. will be taken into account quantitatively. Faradaic efficiences, η_F, were determined from weight loss at rotating (rotation rate = 1500 r.p.m.) and stationary electrodes as a function of alloy composition, concentration of additives in the electrolyte and electrode potential. Practically the same values were obtained from weight loss of the electrodes and from the volume of evolved hydrogen.

For each alloy, faradaic efficiencies were determined with at least one electrolyte composition. We selected the additive amounts (Cl/Zn/In) which yielded not only the lowest overpotentials, but also relatively stable currents at a given potential (i.e. < 50% deviation from the maximum value within 4 h). Depending on alloy and electrolyte composition, the oxidation currents reached, after an induction period of < 1 to several minutes, either a stable or a maximum value. With some alloys, the currents increased steadily with time. The electrode potential of rotating and stationary electrodes was adjusted to reach current densities of $50–200\,mA\,cm^{-2}$. In a few experiments, the electrode potential had to be readjusted after 2 h of operation. The various measurements are summarized in Table 2.

Although the influence of electrolyte composition and electrode potential was not investigated systematically for each alloy, we noticed the following general trends from several test runs: chloride concentrations above 40 mM generally decreased faradaic efficiencies. This finding is in agreement with previously reported results from anodic oxidation of Al(99.5%) [9] in electrolytes containing Zn(II) and In(III) where corrosion rates increased significantly below pH 2 in the presence of high chloride concentrations (2 M NaCl), reaching values of > 75% (η_F < 25%) for zero pH. Similarly to results obtained in slightly acidic (pH 2) saline electrolytes [9, 10], faradaic efficiencies did not depend largely on electrode potential in the current domain of $50–200\,mA\,cm^{-2}$. This observation indicates that the hydrogen evolution rate increases at

*Table 1. Calculated concentrations of fluoride and Al(III) species in 3 M H_2SO_4**

$c_{tot}(F)$/mM	$c_{tot}(Al)$/mM	$c(F^-)$/mM	$c(HF)$/mM	$c(Al^{3+})$/mM	$c(AlF^{2+})$/mM	$c(AlF_2^+)$/mM	$c(AlF_3)$/mM	$c(AlF_4^-)$/mM
40	0	5.7×10^{-3}	40	0	0	0	0	0
60	0	8.5×10^{-3}	60	0	0	0	0	0
160	100	3.8×10^{-3}	27	4.8	58.3	35.5	0.1	0.05
280	200	3.3×10^{-3}	24	12	122	65	0.3	0.1

* Concentrations were calculated from the complex formation constants K_n [44] for the reactions $AlF_{n-1}^{(4-n)+} + F^- \rightarrow AlF_n^{(3-n)+}$ ($n = 1 - 4$): $K_1 \approx 10^{6.5}\,M^{-1}$, $K_2 \approx 10^{5.2}\,M^{-1}$, $K_3 \approx 10^{3.9}\,M^{-1}$, $K_4 \approx 10^{3.4}\,M^{-1}$.

more *positive* potentials. Such a behaviour, named 'negative difference effect', has been reported previously by Despic *et al.* for neutral electrolytes [15, 47].

3.2.1. Rotating Al99.999 electrodes. A faradaic efficiency of 80% was determined from weight loss during anodic oxidation of pure aluminium at -1.15 V (current density of 160 mA cm^{-2}) in 3 M H_2SO_4 containing 40 mM chloride, 10 mM Zn(II) and 1 mM In(III).

3.2.2. Rotating Al–In, Al–Zn/In, Al–Zn/Sn electrodes, influence of chloride-based additives. In the case of Al–In 0.10 with HCl (40 mM) as the only additive, a potential as negative as -1.5 V was sufficient to maintain currents $\geqslant 140$ mA cm^{-2} over a period of 4 h. Under these conditions, faradaic efficiencies were, however, rather low (48–72%) and not as reproducible as with other alloys or additives. When In(III) and/or Zn(II) were added to 3 M H_2SO_4 + 40 mM HCl, the overpotential for comparable anodic currents was higher by 0.1 V, while faradaic efficiencies improved to 80–93% (Table 2).

Table 2. Faradaic efficiencies for anodic aluminium oxidation in 3 M H_2SO_4 with additives

Alloy	*Electrolyte (Cl/Zn/In)*/mM	*Stationary disc electrode*		*Rotating (1500 r.p.m.) disc electrode*	
		i (E/V(Hg/Hg_2SO_4)/mA cm^{-2}	*Faradaic efficiency* 1%	i (E/V(Hg/Hg_2SO_4)/mA cm^{-2}	*Faradaic efficiency* 1%
Al99.999	40/10/1	155 (−1.1)	85	160 (−1.15)	80
Al–In 0.10	40/0/0	0–300 (−1.4)	~30	140–165 (−1.5)	~60
Al–In 0.10	40/80/0	170 (−1.45)	98	200–170 (−1.4)	93
Al–In 0.10	40/80/0.5	155–105 (−1.45)	80	170 (−1.4)	80
Al–Zn/In	40/0/0	145–125 (−1.4)	75	90–120 (−1.4)	84
Al–Zn/In	40/80/0			10 (−1.4), 50–225 (−1.3)*	92
Al–Zn/In	40/80/0.5			175 (−1.4)	93
Al–Zn/In	40/10/1			185–140 (−1.4)	74
Al–Zn/Sn	40/0/0	250 (−1.3), 120 (−1.4)*	81	70–95 (−1.4)	90
Al–Zn/Sn	40/80/0			65–90 (−1.4)	84
Al–Zn/Sn	40/80/0.5			175 (−1.4)	93
Al–Zn/Sn	40/40/0.5			135–230 (−1.4)	94
Al–Ga 0.05	40/80/0.5	130–235 (−1.35), 155 (−1.4)*	48	195–135 (−1.4)	54
Al–Ga 0.10	40/80/0.5	240–105 (−1.4)	30	210–135 (−1.4)	57
Al–Ce 0.05	40/40/0.5	80 (−1.0)	81	110 (−1.1)	81
Al–Ce 0.20	40/10/1	85 (−1.0)	82	270–200 (−1.1)	83
Al–La 0.10	40/10/1	90 (−1.0)	82	145–80 (−1.1)	83
Al–La 0.20	40/10/1	70 (−1.0)	82	225–140 (−1.1)	85
Al–Nd 0.10	40/10/1	0–125 (−1.0)	79	160 (−1.15)	80
Al–Nd 0.29	40/10/1	85 (−1.0)	81	135 (−1.15)	86
Al–Sn 0.50	40/10/1	85 (−1.0)	80	215–180 (−1.1)	92
Al–Sn 0.50	40/10/1			140 (−1.15)	78
Al–Ta 0.10	40/10/1	80 (−1.0)	86	170–100 (−1.15)	95
Al–Ta 0.50	40/10/1	85 (−1.0)	74	225–165 (−1.1)	77
Al–Te 0.014	40/80/0.5			245–185 (−1.1)	85
Al–Te 0.015	40/10/1			215–165 (−1.1)	92
Al–Ti 0.50	40/10/1	80 (−1.0)	79	170–125 (−1.1)	84
Al–Ti 1.2	40/10/1			170–110 (−1.1)	88
Al–Tl 0.086	40/10/1			215–170 (−1.1)	85
Al–Tl 0.16	40/10/1			190–145 (−1.1)	83

* Same measuring time at all potentials

Faradaic efficiencies* of Al–Zn/Sn (84–94%) showed the lowest dependence on the additive combination in the electrolyte. The promising corrosion resistance of Al–Zn/Sn and Al–Zn/In alloys upon anodic oxidation in H_2SO_4 based electrolytes is paralleled by high faradaic efficiencies in alkaline (> 90% at 100 mA cm^{-2} [25]) and neutral electrolytes (up to 98% at 1 mA cm^{-2} [18, 21]).

3.2.3. Rotating Al–Ga electrodes. Al–Ga 0.10 and Al–Ga 0.05 alloys also displayed superactive behaviour in sulphuric acid containing Cl^-, Zn^{2+} and In^{3+} in the electrolyte. At -1.4 V and currents of > 130 mA cm^{-2}, the corrosion rate due to hydrogen evolution was, however, very high ($\eta_F \leqslant 57\%$). High corrosion rates have also been reported for Al–Ga alloys in neutral (in comparison to Al-In alloys, [15]) or alkaline electrolytes (faradaic efficiencies < 12% at 60° C [22]).

3.2.4. Other alloys, rotating electrodes. In comparison to superactive alloys (Al–In, Al–Zn/In, Al–Zn/Sn, Al–Ga), all other alloys had to be tested at more positive potentials, i.e. at -1.1 or -1.5 V for rotating electrodes. Faradaic efficiencies reached values varying from 77 to 95%. In the presence of chloride, Zn(II) and In(III) additives in 3 M H_2SO_4, these binary alloys showed similar or slightly higher currents and faradaic efficiencies as pure aluminium, indicating that the alloying elements Ce, La, Nd, Sn, Ta, Te, Ti or Tl exert no major effect on the electrochemical behaviour in highly acidic electrolytes.

3.2.5. Influence of rotation rate. At rotation rates $\omega \geqslant 1000$ r.p.m., oxidation currents did not depend on ω, while current fluctuations were noted for $\omega \leqslant 600$ r.p.m. during experiments lasting for several hours. The fluctuations were due to accumulation of hydrogen gas at the electrode surface produced by non-faradaic corrosion (in principle, accumulation of hydrogen bubbles could be avoided by employing rotating cone electrodes [48]). At higher rotation rates, however, mass transport was obviously efficient enough to keep the steady-state hydrogen concentration in the diffusion layer low enough that no bubble formation occurred. In order to avoid hydrogen accumulation at stationary disc electrodes, their surface was oriented vertically. The potentials had to be adjusted in some experiments to more positive values (by 0.05–0.2 V) for stationary electrodes in order to obtain comparable currents as with rotating electrodes (50–200 mA cm^{-2}).

The faradaic efficiency for anodic Al–In 0.10 oxidation in 3 M H_2SO_4 + 40 mM HCl was significantly higher for rotating ($\eta_F \approx 60\%$) than for stationary electrodes ($\eta_F \approx 30\%$). Similarly to rotating Al–In 0.10 electrodes in 3 M H_2SO_4 + 40 mM HCl (cf. section 3.2.2.), faradaic efficiencies, determined from several experiments for stationary electrodes, varied by ± 10%. In contrast to most other alloys and additive combinations, surface activation of stationary Al–In 0.10 electrodes in 3 M H_2SO_4 + 40 mM HCl occurred very slowly with anodic currents increasing steadily up to 300 mA cm^{-2} over a period of several hours. When In^{3+} and/or Zn^{2+} were added to the electrolyte, anodic currents at stationary electrodes became significantly more stable and faradaic efficiencies increased (cf. Table 2). In addition, η_F became almost independent of the rotation rate.

Al–Zn/In, Al–Zn/Sn, Al–Ga, Al–Sn, Al–Ta 0.10 yielded slightly higher faradaic efficiencies with rotating electrodes. η_F values of the other alloys tested, i.e. Al–Ce, Al–La, Al–Nd, Al–Ta 0.50, Al–Ti 0.50, were very similar with rotating and stationary anodes.

3.2.6. Influence of fluoride-based additives, rotating disc electrode. Al–Zn/Sn yielded faradaic efficiencies of 78% during anodic oxidation in 3 M H_2SO_4 + 60 mM KF at a potential of -1.3 V (current density of 130–115 mA cm^{-2}), compared to 90% in 3 M H_2SO_4 + 40 mM HCl (Table 2). With 40 mM HCl + 20 mM KF in 3 M H_2SO_4, faradaic efficiency decreased even further to 66% at the same potential but slightly higher currents of 150 mA cm^{-2}. It appears that fluoride increases the corrosion rate in comparison to H_2SO_4 containing only chloride additives (Table 2) and that the combination of fluoride and chloride is even more detrimental. Rather low faradaic efficiencies for aluminium oxidation were also noted by Radosevic *et al.* in neutral NaF/NaCl solutions [45].

3.3. *Surface morphology*

Visual inspection and optical microscopy showed that prolonged anodic oxidation of Al (99.999%) or non-superactive alloys (e.g. Al–Nd) in 3 M H_2SO_4 with chloride, Zn(II) and In(III) additives resulted in rather smooth electrode surfaces (Fig. 6a and b). Generally, a thin dark grey overlayer was formed after rinsing the samples with H_2O and storing them in air. Superactive aluminium alloys on the other hand, yielded a much more heterogeneous surface morphology (Fig. 6c and d), characterized by grooves of up to 1–2 mm depth in the case of Al–Ga (Fig. 6d). While superactive Al–In (Fig. 6c) alloys kept their metallic lustre upon storage in air, Al–Ga became covered with a whitish film.

3.4. *Mechanism of aluminium superactivation*

Aluminium passivation in sulphuric acid due to formation of a porous oxide film is well documented [47, 49, 50] and exploited on a large scale for commercial anodization of aluminium surfaces. In this paper we showed that passivation can be suppressed, even in 3 M H_2SO_4, by suitable electrolyte additives such as halogenides (mainly Cl^-), Zn(II) and In(III). (While localised attack of aluminium oxide by chloride ions, resulting in pits from which active aluminium oxidation can proceed, is understood fairly well [32–40, 47], there is only little information on the mechanistic effects of various metal species either as

* The faradaic efficiency is defined as 100% when 3 electrons per oxidized Al atom and 2 electrons per oxidized Zn atom pass through the electric circuit.

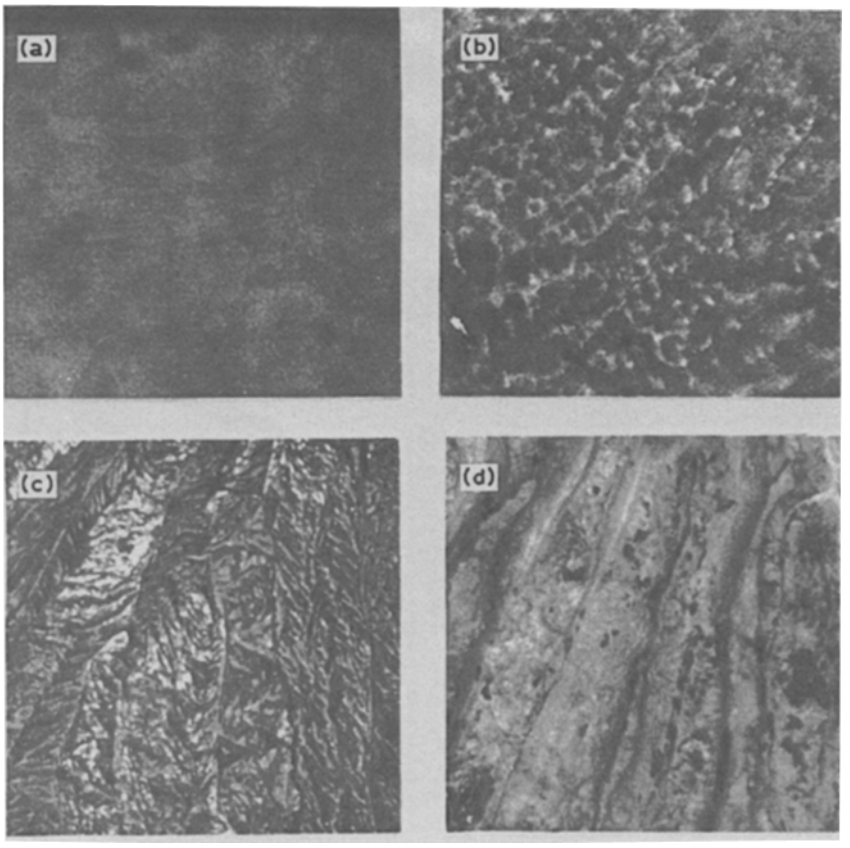

Fig. 6. Optical micrographs of electrode surfaces after potentiostatic anodic polarization of aluminium rotating disc electrodes (1500 r.p.m.) over a period of 4 h in 3 M H_2SO_4 with additives (Cl/Zn/In, concentrations in mM). Al 99.999 (a, 40/10/1), Al–Nd 0.10 (b, 40/10/1), Al–In 0.10 (c, 40/80/0.5), Al–Ga 0.05 (d, 40/80/0.5).

alloying elements or additives in acidic electrolytes. In a previous investigation [9], we showed by X-ray diffraction and SIMS profiling that In and Zn are accumulated at the aluminium surface during anodic oxidation in 2 M NaCl (pH 2) containing 80 mM Zn(II) and 0.5 mM In(III). Preliminary XPS measurements at Al(99.999%) anodized in 3 M H_2SO_4 with chloride, Zn(II) and In(III) additives showed the presence of Zn and In in a hydrated aluminium oxide layer covering the bare metal [51].

Due to the lack of detailed data on the chemical composition of the metal/oxide/electrolye interface in 3 M H_2SO_4, containing additives such as halogenides, Zn(II) or In(III), we will limit our qualitative discussion to some basic thermodynamic considerations. Figure 7 displays the thermodynamic potentials of the relevant electrochemical processes, possibly governing the behaviour of Al–Ga, Al–In, Al–Zn/In and Al–Zn/Sn superactive alloys at pH 0, along with the actual potentials of alloys investigated in this study (at about 100 mA cm^{-2}). Note that the potentials correspond to those of the pure elements and not to those of homogeneous alloys.

The simplified picture (Fig. 7) shows that Sn, In and Ga are electrochemically immune, i.e. cathodically protected against corrosion at potentials < -1.3 V, while Zn is expected to be anodically oxidized at potentials > -1.5 to -1.4 V. Figures 1b and 2b show indeed, that Zn is electroplated at potentials < -1.45 V from 3 M H_2SO_4 containing Zn(II) and anodically oxidized at > -1.45 V, indicating that also the Zn fraction in Al–Zn/In or Al–Zn/Sn alloys can be utilized for the conversion to electricity (cf. footnote in section 3.2.1.).

Upon anodic dissolution of Al(III), some Sn, In and

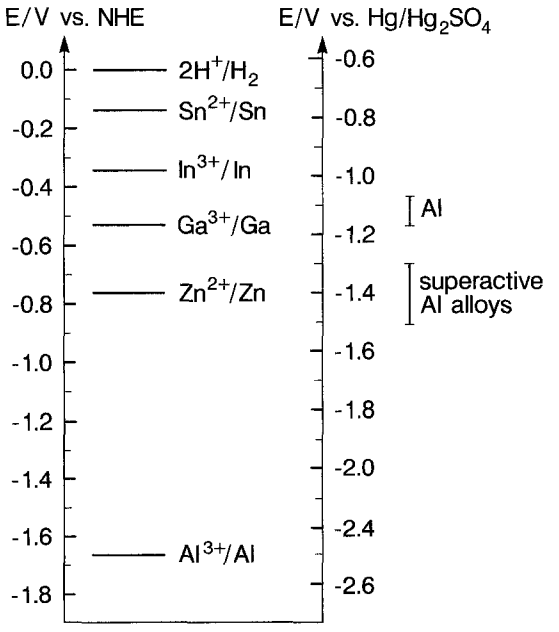

Fig. 7. Standard potentials for electrochemical reactions occurring at superactive alloys in aqueous acidic solutions. NHE: normal hydrogen electrode. Vertical bars mark the potential range where stable anodic currents of about 100 mA cm^{-2} could be maintained at non-superactive (Al) and superactive aluminium alloys in 3 M H_2SO_4 with suitable additives.

Ga species loose their electrical and physical contact to the bulk alloy. These elements are known to corrode in acidic electrolytes at open circuit under concomitant hydrogen evolution [8]. Sn^{2+}, Sn^{4+}, In^{n+} (n = 1–3, [52]) or Ga^{3+} close to the electrode surface may be replated partially on to aluminium, e.g. in pits or be incorporated in the aluminium oxide surface layer. For anodic aluminium oxidation in 2 M NaCl electrolytes (pH 2) containing 0.5 mM In(III) or 0.5 mM Hg(II), however, we showed previously [9, 10] that the In(III) concentration in the electrolyte remained practically constant (although some In species accumulated at the electrode surface), whereas Hg(II) was plated on to aluminium at a rate corresponding to diffusion control.

In analogy to results from alkaline, neutral or slightly acidic electrolytes, Zn, Sn, In or Ga species may be redistributed also in very acidic solutions at grain boundaries, at the interface metal/oxide or within the oxide layer due to electrodeposition or selective incorporation in the oxide/hydroxide layer. This redistribution may influence (i) the kinetics of anodic aluminium oxidation and parasitic hydrogen evolution [16, 17, 19, 22, 24, 26, 53], (ii) the ionic conductivity of the oxide layer and (iii) the surface concentration of halogenides due to specific adsorption. More surface analytical studies are needed to unravel the complex processes occurring upon anodic oxidation of aluminium alloys.

4. Conclusions

The passivating effect of sulphuric acid for anodic oxidation of aluminium was successfully suppressed by adding chloride, Zn(II) or In(III) species to the electrolyte solution. Thus, even highly acidic electrolytes may be utilised for controlled aluminium activation and efficient anodic oxidation in aluminium batteries. Although fluoride additives resulted in even higher electrochemical activity they are not suitable for aluminium/air batteries with acidic electrolytes because of the large, i.e. stoichiometric, quantities required and due to lower faradaic efficiencies in comparison to chlorides.

Al–In, Al–Zn/In and Al–Zn/Sn alloys showed the most promising behaviour for practical applications, i.e. high electrochemical activity (superactivity) and, depending on additive concentrations, faradaic efficiencies of > 90%. Al–Ga alloys, although electrochemically active in acidic electrolytes, are not suitable materials because of the high corrosion rates due to hydrogen evolution. In 3 M H_2SO_4 with chloride, Zn(II) and In(III) additives, Al–Ce, –La, –Nd, –Sn, –Ta, –Te, –Ti and –Tl binary alloys displayed similar electrochemical characteristics as pure aluminium. These alloys require 0.25–0.4 V more positive potentials than superactive alloys, rendering the former materials less interesting for battery purposes. Tests on Al/O_2-batteries with H_2SO_4-based electrolytes and Al–In, Al–Zn/In or Al–Zn/Sn anodes are underway in this laboratory and will be published shortly [31].

Acknowledgement

This work was supported by the Nationaler Energie-Forschung-Fonds (NEFF-Projekt 382). We thank Dr P. Furrer and Dr M. Textor from Alusuisse–Lonza Services AG for providing aluminium alloys and P. Roth for his valuable technical assistance.

References

[1] London Metals Exchange, March (1992).
[2] S. Zaromb, *J. Electrochem. Soc.* **109** (1962) 1125.
[3] B. D. McNicol and D. A. J. Rand (Eds), Power Sources for Electric Vehicles, in 'Studies in Electrical and Electronic Engineering', Vol. 2, Elsevier, Amsterdam (1984) p. 602.
[4] J. Hunter, G. Scamans and J. Sykes, in 'Power Sources 13: Research and Development in Non-Mechanical Electric Power Sources', (edited by T. Keily and B. W. Baxter), 17th International Power Sources Symposium, Bournemouth (1991) p. 193.
[5] D. M. Drazic, A. R. Despic, S. Zecevic and M. Atanackovic, 'Power Sources 7', 11th International Symposium Sources Symposium, Brighton (1978) p. 353.
[6] M. Ritschel and W. Vielstich, *Electrochim. Acta* **24** (1979) 885.
[7] E. Budevski, I. Iliev, A. Kaisheva, A. Despic and K. Krsmanovic, *J. Appl. Electrochem.* **19** (1989) 323.
[8] 'Atlas of Electrochemical Equilibria in Aqueous Solutions', (edited by M. Pourbaix), 2nd ed., NACE, Houston, TX, Cebelcor, Brussels (1974).
[9] G. Buri, W. Luedi and O. Haas, *J. Electrochem. Soc.* **136** (1989) 2167.
[10] J.-F. Equey, S. Müller, J. Desilvestro and O. Haas, *J. Electrochem. Soc.* **139** (1992) 1499.
[11] J.-F. Equey, S. Müller, A. Tsukada and O. Haas, *J. Appl. Electrochem.* **19** (1989) 65.
[12] *ibid.* **19** (1989) 147.
[13] A. V. Kuz'mina, *J. Appl. Chem. USSR* **43** (1970) 902.
[14] J. T. Reding and J. J. Newport, *Materials Protection* **5** (Dec.) (1966) 15.
[15] A. R. Despic, D. M. Drazic, M. M. Purenovic and N. Cikovic, *J. Appl. Electrochem.* **6** (1976) 527.
[16] T. Våland and G. Nilsson, *Corros. Sci.* **17** (1977) 931.
[17] M. C. Reboul and M. C. Delatte, *Materials Performance* **19**(5), (1980) 35.
[18] M. C. Reboul, Ph. Gimenez and J. J. Rameau, *Corrosion* **83** (1983) Paper No. 214.
[19] *Idem, Corrosion-NACE* **40** (1984) 366.
[20] Y. Hori, J. Takao and H. Shomon, *Electrochim. Acta* **30** (1985) 1121.
[21] J. C. Lin and H. C. Shih, *J. Electrochem. Soc.* **134** (1987) 817.
[22] C. D. S. Tuck, J. A. Hunter and G. M. Scamans, *ibid.* **134** (1987) 2970.
[23] D. D. Macdonald, K. H. Lee, A. Moccari and D. Harrington, *Corros. Sci.* **44** (1988) 652.
[24] D. D. Macdonald, S. Real and M. Urquidi-Macdonald, *J. Electrochem. Soc.* **135** (1988) 2397.
[25] A. Sheik Mideen, M. Ganesan, M. Anbukulandainathan, K. B. Sarangapani, V. Balaramachandran, V. Kapali and S. Venkatakrishna Iyer, *J. Power Sources* **27** (1989) 235.
[26] W. Wilhelmsen, T. Arnesen, O. Hasvold and N. J. Storkersen, *Electrochem. Acta* **36** (1991) 79.
[27] G. D. Davis, W. C. Moshier, T. L. Fritz and G. O. Cote, *J. Electrochem. Soc.* **137** (1990) 422.
[28] H. Yoshioka, Q. Yan, H. Habazaki, A. Kawashima, K. Asami and K. Hashimoto, *Corros. Sci.* **31** (1990) 349.
[29] Q. Yan, H. Yoshioka, H. Habazaki, A. Kawashima, K. Asami and K. Hashimoto, *Corros. Sci.* **32** (1991) 327.
[30] O. Haas, S. Müller, F. Holzer and J. Desilvestro, *Swiss Patent CH 679 438 A5* (1992).
[31] S. Müller, F. Holzer, J. Desilvestro and O. Haas, *J. Appl. Electrochem.*, in preparation.
[32] S. Dallek and R. T. Foley, *J. Electrochem. Soc.* **123** (1976) 1775.
[33] R. M. Stevanovic, A. R. Despic and D. M. Drazic, *Electrochim. Acta* **33** (1988) 397.

[34] P. L. Cabot, F. A. Centellas, J. A. Garrido, E. Perez and H. Vidal, *ibid.* **36** (1991) 179.
[35] A. A. Mazhar, W. A. Badawy and M. M. Abou-Romia, *Surf. Coat. Technol.* **29** (1986) 335.
[36] R. Narayan and K. P. Sherif, *Indian J. Technol.* **24** (1986) 515.
[37] S. Bourkane, C. Gabrielli, M. Keddam, O. Haas and M. Mathias, *Mater. Sci. Forum* **44 & 45** (1989) 403.
[38] T. R. Beck, *Electrochim. Acta* **33** (1988) 1321.
[39] B. J. Wiersma and K. R. Hebert, *J. Electrochem. Soc.* **138** (1991) 48.
[40] L. Tomcsanyi, K. Varga, I. Bartik, G. Horanyi and E. Maleczki, *Electrochim. Acta* **34** (1989) 855.
[41] J. Painot and J. Augustynski, *ibid.* **20** (1975) 747.
[42] Lj. D. Atanasoska, D. M. Drazic, A. R. Despic and A. Z-alar, *J. Electroanal. Chem.* **182** (1985) 179.
[43] P. A. Wycliffe and W. Halliop, in 'Extended Abstracts', Vol. 90–1, Electrochem. Soc., Montreal, Québec (1990) p. 9.
[44] E. Hoegfeldt, 'Stability Constants of Metal–Ion Complexes, Part A: Inorganic Ligands', Intern. Union of Pure and Appl. Chemistry, Pergamon Press, Oxford (1982).
[45] J. Radosevic, Z. Mentus, A. Djordjevic, and A. R. Despic, *J. Electroanal. Chem.* **193** (1985) 241.
[46] 'Handbook of Chemistry and Physics', (edited by R. C. Weast), 55th ed., CRC Press, Ohio (1974–1975).
[47] A. R. Despic and V. Parkhutik, in 'Modern Aspects of Electrochemistry', (edited by J. O'M. Bockris *et al.*), Vol. 20, Plenum Press, New York and London (1990) p. 401.
[48] E. Kirowa-Eisner and E. Gileadi, *J. Electrochem. Soc.* **123** (1976) 25.
[49] T. P. Hoar and J. Yahalom, *ibid.* **110** (1963) 614.
[50] B. Schnyder and R. Kötz, *J. Electroanal. Chem.*, in press.
[51] R. Kötz, unpublished results.
[52] R. Piercy and N. A. Hampson, *J. Appl. Electrochem.* **5** (1975) 1.
[53] K. Nisancioglu, L. Odden and A. P. Grande, in 'Proceedings of the 2nd Symp. on Electrode Materials and Processes for Energy Conversion and Storage', (edited by S. Srinivasan and S. Wagner), Vol. 87-12, Electrochemical Society, Philadelphia (1987) p. 499.
[54] D. S. Keir, M. J. Pryor and P. R. Sperry, *J. Electrochem. Soc.* **114** (1967) 777.